Journal of
Computational and Theoretical Nanoscience
Vol. 7, 1294–1298, 2010

Molecular Dynamics Simulations of Stretching, Twisting and Fracture of Super Carbon Nanotubes with Different Chiralities: Towards Smart Porous and Flexible Scaffolds

Vitor R. Coluci[1] and Nicola M. Pugno[2,*]

[1] *School of Technology, University of Campinas, Limeira-SP, 13484-332, Brazil*
[2] *Laboratory of bio-inspired Nanomechanics "Giuseppe Maria Pugno", Department of Structural Enginnering, Politecnico di Torino, Torino, 10129, Italy*

The mechanical properties of ordered single walled carbon nanotube networks in tubular forms (super carbon nanotubes–STs) are investigated using classical molecular dynamics simulations based on reactive empirical bond-order potential. During tensile deformations the shape and size of pores in ST sidewalls can be modified providing a way to vary the accessible channels to and from the inner parts of STs. The investigated STs presented values of fracture toughness, fracture energy, and dissipated energy that are about 5, 8, and 2 times smaller than the ones presented by the constituent (8,0) single walled carbon nanotube, respectively. Simulations indicate that these networks are also very flexible under torsional loads, mainly zigzag STs. Based on the predicted mechanical properties, STs may represent new candidates for novel porous, flexible, and high strength nanomaterials, e.g., smart porous and flexible scaffolds for the regenerative medicine.

Keywords: Ordered Carbon Nanotube Networks, Super-Nanotubes, Molecular Dynamics, Stretching, Twisting, Fracture, Smart, Porosity, Flexibility, Scaffolds, Regenerative Medicine.

1. INTRODUCTION

Carbon nanotubes, possessing extremely high strength and stiffness, are ideal candidates as nanofiber-reinforcements.[1] Many attempts have been made to develop procedures to controllably assemble large number of single walled carbon nanotubes (SWCNTs) in terms of position and orientation. These procedures would allow the fabrication of ordered SWCNT networks and their use in designing of new materials with desirable electronic and mechanical properties. Many research groups have been working on the production of carbon nanotube networks.[2–8] Snow et al. have demonstrated the capability of random carbon nanotube networks to function as transistors[3] and chemical sensors.[4] Many companies such as DuPont, IBM, Intel, Motorola and Samsung are currently doing research in order to develop applications based on carbon nanotube networks.[9] Recently, Hall et al. showed that carbon nanotube networks can exhibit unusual mechanical properties such as negative Poisson's ratio, i.e., a lateral dimension expands during stretching.[10]

With the purpose of producing *ordered* carbon nanotube networks, Diehl et al. have developed a technique that applies electric field to controllably arrange nanotubes on a "crossbar" configuration on silicon oxide surfaces.[7] Exploring the morphology of silicon carbide surfaces, Derycke et al. were able to produce ordered nanotube networks with "hexagonal" and "crossbar" arrangements.[2] These nanotubes were produced after the heating of the surface over 1500 °C in vacuum. Scanning tunneling microscopy images indicated that the nanotube organization follows the surface morphology. This technique of using surfaces has been applied by other groups to produce highly aligned carbon nanotubes on the surface[11] and networks composed exclusively by SWCNT.[12] In those networks, the nanotubes are weakly bonded by van der Waals interactions with the nanotubes radially deformed at the junctions (Fig. 1(a)).

The ultimate arrangement involving SWCNTs would be the one where isolated SWCNTs are covalently connected by using X-, Y-, or T-shaped junctions, forming a

*Author to whom correspondence should be addressed.

 1546-1955/2010/7/1294/005 doi:10.1166/jctn.2010.1483

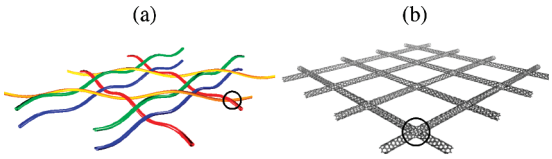

Fig. 1. Schematic view of (a) a random and (b) an ordered carbon nanotube network. In this example, the elements of the random network are weakly bonded at the junctions (indicated by the black circles) while the ones of the ordered mat are covalently connected.

highly-ordered network (Fig. 1(b)). The mechanical properties of these ideal networks were investigated by using molecular dynamics simulations.[13] The simulations indicated that these ordered networks become stiffer under large displacements, due to the activation of a rope-like behaviour. This is associated to the high Young's modulus presented by the nanotubes (∼1 TPa) and due to the difference of the effective spring constants related to the nanotube bending at stretching.

Several biological applications of ordered SWCNT networks are envisioned, for example, as scaffolds in the regenerative medicine. In particular, adult stem cells are a promising therapy for stroke and other brain injuries, but they tend to migrate to health regions of the brain. What is needed is an anchor to keep stem cells fixed to the damaged areas, where they can then differentiate into working neurons. The efficacy of carbon nanotubes have already been demonstrated in this context,[14] not only acting as scaffolds, helping stem cells stay rooted to diseased areas, but also playing an active role in turning stem cells into neurons. In general, scaffolds are becoming very popular in medicine, and the main attribute that they must possess is of resembling the tissue to be repaired in terms of stiffness and topology, to promote regeneration. While such parameters cannot be smartly controlled in nanotubes, they can in ordered SWCNT networks. Surprisingly, the differentiation itself is expected to be mainly a function of stiffness[15] and topology (here mainly porosity).[16] Controlling porosity and flexibility, in addition, play a key role also for optimal drug delivering in nanovector therapeutics[17] and thus we expect ordered SWCNT networks to be multifunctional smart scaffolds and nanovectors. Gecko-inspired self-adhesive bandages are also envisioned for biomedical applications[18] mimicking the smart adhesion of geckos,[19–21] discussed also in large size-scale "spiderman" tissues.[22, 23]

Accordingly, in this work, we investigate the behaviour of ordered single walled carbon nanotube networks using atomistic simulations. The rupture process is analyzed in networks formed by rolling up planar mats during tensile and torsional deformation regimes. These rolled up mats were named "super" carbon nanotubes (STs)[24] and, similarly to a (N, M) SWCNT,[1] (N, M) ST with different chiralities can be constructed. The nomenclature $[N, M]@(n, m)$ indicates a ST of chirality (N, M) constructed with (n, m) SWNTs.

2. MOLECULAR DYNAMICS

The rupture and mechanical properties of ordered SWCNT networks have been preliminary investigated using molecular dynamics simulations in Ref. [25]. The adaptive intermolecular reactive empirical bond-order (AIREBO) potential developed by Stuart et al.[26] was used to model carbon–carbon interactions. AIREBO is similar to the reactive potential developed by Brenner[27] but it incorporates by suitable modifications the non-bonded interactions through an adaptative treatment of the intermolecular interactions. These kinds of reactive potentials have been proved to be accurate to describe carbon nanotube deformations under mechanical strain.[28] Due to the possibility of modeling bond-breaking, reactive force fields, such as AIREBO and ReaxFF,[29] have been used on studies involving the rupture process of covalent nanomaterials. During the molecular dynamics simulations, Newton's equations of motion were integrated with a third-order Nordisieck predictor corrector algorithm[30] using a time step of 0.5 fs.

Following this procedure we have here carried out simulations of tensile tests in situations of impact load, i.e., the atoms on the ST extremities were moved along the axial directions with a speed of 10 m/s (Fig. 2(a)). The strain rate used here is very high if compared to real strain rate values. The use of such high values is due to computational limitations, since a very small time step is necessary during integration of Newton's equations in order to describe the main atomic motions. In order to obtain results for much lower and thus realistic strain rates, multiscale modeling approaches should be applied. For instance, Ackbarow and Buehler[31] have combined atomistic simulations and continuum theory

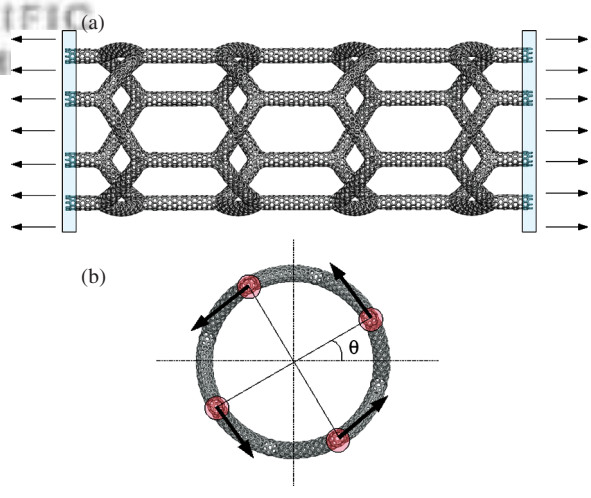

Fig. 2. A carbon nanotube network (super-nanotube, ST) under (a) tensile and (b) torsional strains. Longitudinal (a) and cross section (b) views of a [4,0]@(8,0) ST. In the ST construction SWCNTs are connected by Y-like junctions. The atoms in the ST extremities (filled boxes, (a)) are moved with a constant speed during tensile tests. Filled discs (b) represent the cross-sectional ST area.

to investigate the tensile properties of Vimentin coiled-coil alpha-helical dimmers, which allowed to extrapolate their results to strain rates comparable to those found in experiments.

Torsional strains were applied through the rotation of the atoms on the ST extremities (radius fixed, Fig. 2(b)) in a rate of 1° per 1000 time steps (3.5×10^{-5} rad/fs). In order to investigate thermal effects on the tensile behaviour of STs, the Berendsen thermostat[32] was applied to all remaining atoms. Tensile and torsional behaviours at 300 K were analysed. We have investigated zigzag $[N, 0]$@(8,0) and armchair $[M, M]$@(8,0) STs with $4 \leq N \leq 6$ and $4 \leq M \leq 6$, with initial tube lengths ranging from 8.6 to 35.2 nm, corresponding to two ST unit cells.

3. RESULTS

Figure 3 shows the tensile behavior for a zig-zag and an armchair ST. The rupture in zigzag STs occurs at breaking strains at about 28–30% (Fig. 3(a)). This value is close to that obtained for a (8, 0) SWCNT. The ST deformation is mainly due to angle changing rather than SWCNT stretching, as confirmed by the observed hyper-elasticity due to a fishing-net-like behaviour. During the tensile deformation, the angles between SWCNTs in the ST structures are changed and the stress concentration is mainly observed at the junctions. The ST rupture occurs near the junctions close to the ST extremities where different SWCNTs break approximately at the same time, causing an abrupt decrease of the strain energy. Thus, due to the large changes in the angles between SWCNTs, the rupture happens before the occurrence of an effective stretching of SWCNTs. In fact, by increasing the zigzag ST radius, the breaking strain is shifted to a higher value than that found in a zigzag ST with a smaller radius.

For the armchair ST the rupture occurs not abruptly, as in the zigzag case, but in small steps through a quantized breaking of the junctions. This behaviour can be seen in the strain energy evolution shown in Figure 3(b), where many decreasing steps of the strain energy are observed and associated with local ruptures on the ST structure.

The key points related to the different behaviours presented by zigzag and armchair STs are the junctions and their arrangement in the STs. We have associated the deformation behaviour of STs with two main mechanisms. The first one is associated with the SWCNT stretching, dictated by the SWCNT mechanical property. The second one is due to the deformation at the junctions, i.e., changes in the angle of the junctions. These changes are relatively easier to occur than the SWCNT stretching, due to the high value of the SWCNT Young's modulus. Consequently, for cases where the arrangement of junctions in the ST facilitates the deformation of the first type in a tensile test, the ST will present a tensile strength and breaking strain similar to the constituent SWCNT. It will not be exactly the same due to the effect of the second type of deformation. This is the case for the [4,0]@(8,0) STs, Figure 3(a). On the other hand, when the second type of deformation is favoured during the tensile test, due to the arrangement of the junctions, the angle changes become more relevant than the SWCNT stretching, as in the case of the [4,4]@(8,0) STs (Fig. 3(b)).

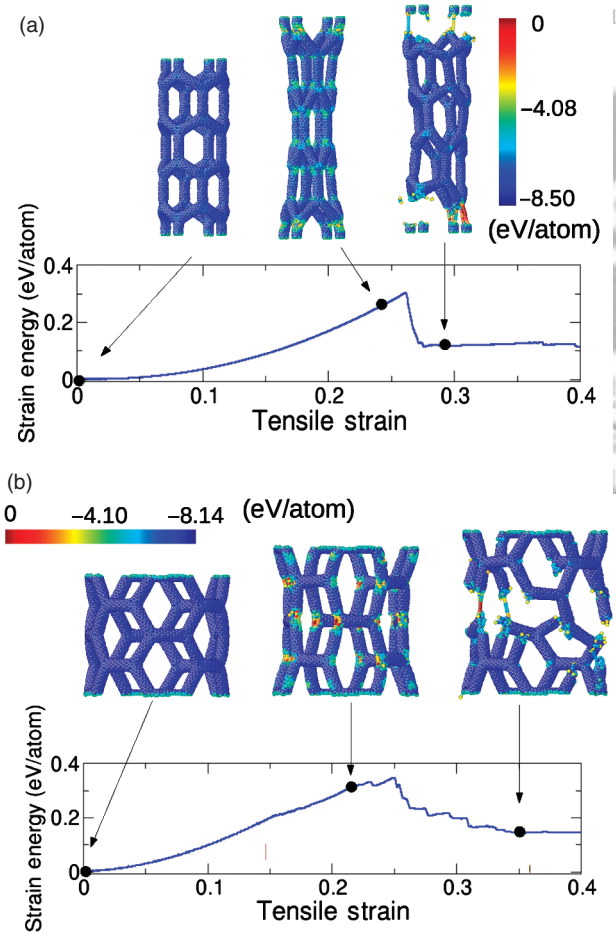

Fig. 3. Behaviour of the strain energy as function of the tensile strain for the (a) [4,0]@(8,0) ST with $R = 2.72$ nm and (b) [4,4]@(8,0) ST with $R = 4.74$ nm at 300 K. Snapshots of the simulations are presented for specific tensile strains. Atoms are coloured according to their potential energy.

Table I. Atomistic results for the tensile strength σ_c, breaking strain ε_c, fracture toughness (K_c), fracture energy (G_c), and dissipated energy per unit mass (D_c) at 300 K for zig-zag and armchair STs.

Structure	Radius (nm)	σ_c (GPa)	ε_c	K_c (MPa m$^{1/2}$)	G_c (N/m)	D_c (kJ/g)
(8,0)	0.31	92.6	0.28	25.6	876	10.7
[4, 0]@(8, 0)	2.72	79.2	0.26	6.8	160	5.5
[4, 0]@(8, 0)	3.66	77.9	0.27	5.8	188	4.9
[4, 4]@(8, 0)	4.74	55.5	0.22	6.2	106	6.5
[4, 4]@(8, 0)	6.36	36.5	0.15	4.5	81	3.6

Table I summarizes some of the mechanical properties of zig-zag and armchair STs investigated here. We can use these data to estimate the toughness presented by STs. Using the estimated reduction (<50%) of dissipated energy per unit mass presented by STs compared to (8,0) SWCNTs at 300 K and the value of carbon nanotube fibres comprising SWCNTs in a polymer matrix (570 J/g),[33] that is higher than that presented by spider dragline silk (165 J/g)[24] and Kevlar (33 J/g),[34] we can roughly estimate a real toughness value for STs as $\sim 570/2 = 285$ J/g. Therefore, our calculations, resulting in strengths of several gigapascals and toughness of ∼280 J/g, suggest that super-composites based on STs[35, 36] could be competitive with super-tough carbon nanotube fibres (strength of 1.8 GPa and toughness of 570 J/g).[33] The observed fracture mechanisms are peculiar of the nanoscale and differ with respect to those typically arising at size-scales larger than the micrometer.[37]

The torsional behaviour of some STs is shown in Figures 4 and 5. From our simulations we noticed that zigzag STs can achieve larger torsional strain before breaking compared to armchair STs. For the [4,0]@(8,0) ST with a radius of 2.72 nm we observed a collapse of the structure when the imposed torsional angle θ is about 45° (see Fig. 5), which is associated to the first decrease on the strain energy.

As the radius increases the angle where collapse occurs is shifted to large values. Similarly to the case of tensile strains, the rupture for torsional strains occurs mainly on the regions of the nanotube junctions as we can see for the [4,4]@(8,0) ST in Figure 5. The breaking of the tube due to torsional strain occurs at about 45° and 137° for [4,4]@(8,0) and [6,0]@(8,0) ($R = 4.10$ nm) STs, respectively. On the other hand, for the [4,0]@(8,0) STs the rupture was observed for values above 270°. These results indicate that STs also present high flexibility under torsional loads. We obtained the following values for the second derivative of the torsional strain energy with respect to the rotation angle (in eV/atom/rad^2): 0.12, 0.08, 0.13, and 1.10, for the [4,0]@(8,0) ($R = 2.72$ nm), [4,0]@(8,0) ($R = 3.66$ nm), [6,0]@(8,0) ($R = 4.10$ nm), and [4,4]@(8,0) ($R = 4.74$ nm), respectively.

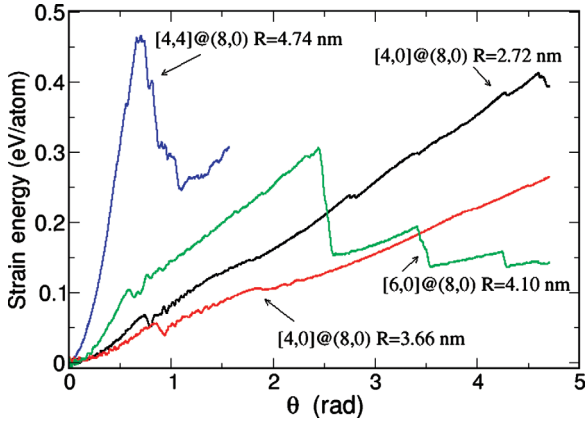

Fig. 4. Behaviour of the torsional strain energy as function of the rotation angle θ for different STs for 300 K.

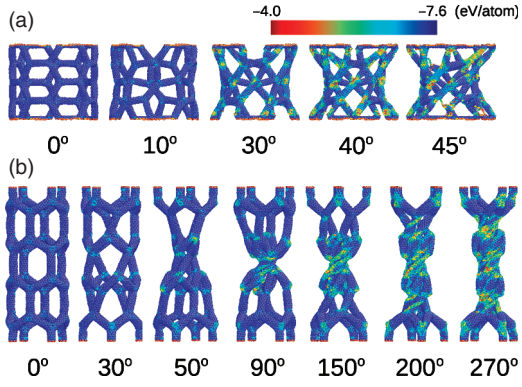

Fig. 5. Snapshots of the torsional behavior for different θ angles for (a) [4,4]@(8,0) and (b) [4,0]@(8,0) with radius $R = 2.72$ nm (see Fig. 4). Atoms are coloured according to their potential energy.

4. CONCLUSIONS

The mechanical properties of the single walled carbon nanotube networks arranged in a form of tubes (STs) are investigated using classical molecular dynamics simulations based on reactive empirical bond-order potential. From tensile tests of impact loads, we have found that STs are more flexible than the SWCNT used to form them but, in some cases, they show comparable tensile strengths. During tensile deformations the shape and aperture of pores in ST sidewalls can be modified providing a way to vary the accessible channels to the inner parts of STs through the application of mechanical loads. Torsional tests indicated ST chirality dependence on the breaking torsional strain values. The ST rupture occurs basically at regions near the SWCNT junctions and it is influenced by the ST chirality. The investigated STs presented values of fracture toughness, fracture energy, and dissipated energy that are about 5, 8, and 2 times smaller than the ones presented by the constituent (8,0) SWCNT, respectively. Simulations indicated that these networks are also very flexible under torsional loads, mainly zigzag STs. Based on the predicted mechanical properties, STs may represent new candidates for novel porous, flexible, and high strength materials, e.g., towards smart porous and flexible scaffolds.

Acknowledgments: Vitor R. Coluci acknowledges the financial support from the Brazilian agency FAPESP (grant 2007/03923-1). Nicola M. Pugno acknowledges the financial support from the Piemonte Region, "Converging Technologies", Biotechnology–Nanotechnology, METREGEN 2008, "Metrology on a cellular and macromolecular scale for regenerative medicine".

References

1. R. H. Baughman, A. A. Zakhidov, and W. A. de Heer, *Science* 297, 787 **(2002)**.
2. V. Derycke, R. Martel, M. Radosavljevic, F. M. Ross, and Ph. Avouris, *Nano Lett.* 2, 1043 **(2002)**.
3. E. S. Snow, J. P. Novak, P. M. Campbell, and D. Park, *Appl. Phys. Lett.* 82, 2145 **(2003)**.
4. E. S. Snow, J. P. Novak, M. D. Lay, E. H. Houser, F. K. Perkins, and P. M. Campbell, *J. Vac. Sci. Technol. B* 22, 1990 **(2004)**.
5. Y. J. Jung, Y. Homma, T. Ogino, Y. Kobayashi, D. Takagi, B. Wei, R. Vajtai, and P. M. Ajayan, *J. Chem. Phys. B* 107, 6859 **(2003)**.
6. A. M. Cassell, G. C. McCool, H. T. Ng, J. E. Koehne, B. Chen, J. Li, J. Han, and M. Meyyappan, *Appl. Phys. Lett.* 82, 817 **(2003)**.
7. M. R. Diehl, S. N. Yaliraki, R. A. Beckman, M. Barahoma, and J. R. Heath, *Angew. Chem.* 114, 363 **(2002)**.
8. S. M. Huang, B. Maynor, X. Y. Cai, and J. Liu, *Adv. Mater.* 15, 1651 **(2003)**.
9. G. Gruner, *Scientific American* 296, 76 **(2007)**.
10. L. J. Hall, V. R. Coluci, D. S. Galvão, M. E. Kozlov, M. Zhang, S. O. Dantas, and R. H. Baughman, *Science* 320, 504 **(2008)**.
11. H. Ago, K. Nakamura, K. Ikeda, N. Uehara, N. Ishigami, and M. Tsuji, *Chem. Phys. Lett.* 408, 433 **(2005)**.
12. A. Ismach, D. Kantorovich, and E. Joselevich, *J. Am. Chem. Soc.* 127, 11554 **(2005)**.
13. A. Ismach and E. Joselevich, *Nano Lett.* 6, 1706 **(2006)**.
14. V. R. Coluci, S. O. Dantas, A. Jorio, and D. S. Galvão, *Phys. Rev. B* 75, 075417 **(2007)**.
15. M. A. Correa-Duarte, N. Wagner, J. Rojas-Chapana, C. Morsczeck, M. Thie, and M. Giersig, *Nano Lett.* 4, 2233 **(2004)**.
16. A. J. Engler, S. Sen, H. L. Sweeney, and D. E. Discher, *Cell* 126, 677 **(2006)**.
17. S. Oh, K. S. Brammer, Y. S. J. Li, D. Teng, A. J. Engler, S. Chien, and S. Jin, *Proc. Natl. Acad. Sci USA* 106, 2130 **(2009)**.
18. N. Pugno, *J. Phys. Cond. Mat.* 20, 474205 **(2008)**.
19. A. Mahdavi, L. Ferreira, C. Sundback, J. W. Nichol, E. P. Chan, D. J. D. Carter, C. J. Bettinger, S. Patanavanich, L. Chignozha, E. Ben-Joseph, A. Galakatos, H. Pryor, I. Pomerantseva, P. T. Masiakos, W. Faquin, A. Zumbuehl, S. Hong, J. Borenstein, J. Vacanti, R. Langer, and J. M. Karp, *Proc. Natl. Acad. Sci. USA* 105, 2307 **(2008)**.
20. E. Lepore, F. Antoniolli, M. Buono, S. Brianza, A. Carpinteri, and N. Pugno, *J. Nanomater.* 194524, (5pp) **(2008)**.
21. N. Pugno and E. Lepore, *Biosystems* 94, 218 **(2008)**.
22. N. Pugno and E. Lepore, *J. Adhesion* 84, 949 **(2008)**.
23. N. Pugno, *J. Phys. Cond. Mat.* 19, 395001 **(2009)**.
24. N. Pugno, *Nano Today* 3, 35 **(2008)**.
25. V. R. Coluci, D. S. Galvão, and A. Jorio, *Nanotechnology* 17, 617 **(2006)**.
26. D. C. Rapaport, The Art of Molecular Dynamics Simulation, Cambridge University, Cambridge **(1995)**.
27. S. J. Stuart, A. B. Tutein, and J. A. Harrison, *J. Chem. Phys.* 112, 6472 **(2000)**.
28. D. W. Brenner, *Phys. Rev. B* 42, 9458 **(1990)**.
29. B. I. Yakobson, C. J. Brabec, and J. Bernholc, *Phys. Rev. Lett.* 76, 2511 **(1996)**.
30. M. J. Buehler, A. C. T. van Duin, and W. A. Goddard, III, *Phys. Rev. Lett.* 96, 095505 **(2006)**.
31. M. P. Allen and F. J. Tildesley, Computer Simulation of Liquids, Oxford University Press, New York **(1987)**.
32. T. Ackbarow and M. J. Buehler, *J. Mater. Sci.* 42, 8771 **(2007)**.
33. H. J. C. Berendsen, J. P. M. Postma, D. A. van Gunsteren, and J. R. Haak, *J. Chem. Phys.* 81, 3684 **(1984)**.
34. A. B. Dalton, S. Collins, R. Munhoz, J. M. Razal, F. H. Ebron, J. P. Ferraris, J. N. Coleman, B. G. Kim, and R. H. Baughman, *Nature* 423, 703 **(2003)**.
35. F. Vollrath and F. P. Knight, *Nature* 410, 541 **(2001)**.
36. N. M. Pugno, *Nanotechnology* 17, 5480 **(2006)**.
37. V. R. Coluci, N. M. Pugno, S. O. Dantas, D. S. Galvão, and A. Jorio, *Nanotechnology* 18, 335702 (7pp) **(2007)**.
38. N. Pugno, B. Peng, and H. D. Espinosa, *Int. J. Solids and Structures* 42, 647 **(2004)**.

Received: 23 April 2009. Accepted: 10 July 2009.